Journal of Sound and Vibration (1997) **200**(1), 83–103

A MODAL ANALYSIS OF WHOLE-BODY VERTICAL VIBRATION, USING A FINITE ELEMENT MODEL OF THE HUMAN BODY

S. KITAZAKI AND M. J. GRIFFIN

Human Factors Research Unit, Institute of Sound and Vibration Research, University of Southampton, Southampton SO17 1BJ, England

(*Received* 12 *December* 1995, *and in final form* 30 *July* 1996)

A two-dimensional model of human biomechanical responses to whole-body vibration has been developed, by using the finite element method. Beam, spring and mass elements were used to model the spine, viscera, head, pelvis and buttocks tissue in the mid-sagittal plane. The model was developed by comparison of the vibration mode shapes with those previously measured in the laboratory. At frequencies below 10 Hz, the model produced seven modes which coincided well with the measurements. The principal resonance of the driving point response at about 5 Hz consisted of an entire body mode, in which the head, spinal column and the pelvis move almost rigidly, with axial and shear deformation of tissue beneath the pelvis occurring in phase with a vertical visceral mode. The second principal resonance at about 8 Hz corresponded to a rotational mode of the pelvis, with a possible contribution from a second visceral mode. A shift of the principal resonance of the driving point response, when changing posture, was achieved only by changing the axial stiffness of the buttocks tissue. It is suggested that an increase in contact area between the buttocks and the thighs and the seat surface, when changing posture from erect to slouched, may decrease the axial stiffness beneath the pelvis, with a non-linear force–deflection relationship of tissue resulting in decreases in the natural frequencies. A change in posture from erect to slouched also increased shear deformation of tissue beneath the pelvis in the entire body mode, and the natural frequency was decreased as a result of the much lower shear stiffness of tissue compared to the axial stiffness.

1. INTRODUCTION

Experimental studies exhibit a consistent pattern for the vertical response of the seated human body exposed to whole-body vertical vibration. A principal resonance has consistently been found between 4 and 6 Hz in the driving point impedance or apparent mass (e.g., by Coermann [1], and Fairley and Griffin [2]), and in seat-to-head transmissibilities (e.g., by Coermann [1]) and seat-to-spine transmissibilities (e.g., by Panjabi *et al*. [3]). Another resonance between 8 and 12 Hz has been found in some investigations (e.g., by Coermann [1], and Fairley and Griffin [2]), but it is less clear and the variability between investigations and between subjects is larger. It has been reported that the frequency of the principal resonance tends to decrease when subjects change their postures from erect to relaxed (e.g., by Coermann [1], and Fairley and Griffin [2]).

0022–460X/97/060083 + 21 $25.00/0/sv960674

The body motions occurring at the resonances have been hypothesized by some workers so as to identify the major contributors to the resonances. Hagena *et al*. [4] compared vertical transmissibilities from the vibrator platform to the spine and from the sacrum to the spine in both sitting and standing positions. They suggested that the principal resonance found at 4–5 Hz corresponded to motion of the entire body and the second resonance at 7–10 Hz corresponded to motion of the spinal column. From an observation of the spinal motion both in the vertical and fore-and-aft directions, Sandover and Dupuis [5] hypothesized that the principal resonance found at 4 Hz did not relate to buttocks compression but related to bending motion of the lumbar spine which was caused by pelvic rotation. Hinz *et al*. [6] found that a flexion and an extension of the spine at 4·5 Hz were accompanied by downwards and upwards motion of the whole body respectively. The authors suggested that vertical motion of the body parts above the vertebral level L3–L4 seemed to be the main cause for the bending motion of the lumbar spine and the rotation of the pelvis might be a secondary effect.

Many different models of biomechanical responses to whole-body vibration have been proposed for different purposes, with different idealizations of the body structure. The models can be categorized into three types: lumped parameter models, continuum models and discrete models. In the lumped parameter models, the mass of the body structure is concentrated into a few lumped masses interconnected by springs and dampers. The development of such models started with single-degree-of-freedom models (e.g., those of Latham [7] and Payne [8]); successive investigators increased the number of degrees of freedom (e.g., Suggs *et al*. [9], and Payne and Band [10]). The majority of lumped parameter models are one-dimensional.

Discrete models and continuum models are both distributed parameter models. The discrete models treat the spine as a layered structure of rigid elements, representing the vertebral bodies, and deformable elements representing the intervertebral discs. The continuum models treat the spine as a homogeneous rod or beam. Toth [11] modelled each vertebra separately in an eight-degree-of-freedom non-linear discrete model. Orne and Liu [12] found that mass centres of the torso segments are located anterior to the spine due to the presence of the rib cage and the viscera. They developed a two-dimensional discrete model which included the initial curvature of the spine and the eccentric inertial loading of the torso. Belytschko *et al*. [13] developed a highly anatomical three-dimensional discrete model which consisted of the spine, ribs, head, pelvis and the viscera. Belytschko and Privitzer [14] subsequently developed this model into a series of other models with a range of complexities. The development of continuum models has followed a similar history.

Kitazaki and Griffin [15] extracted the vibration mode shapes of the body in the mid-sagittal plane, using experimental modal analysis (see the Appendix). The effect of changing posture, which was defined by the spinal curvature and the pelvic angle, was also studied. The results showed that the modes found at frequencies below 10 Hz contained bending deformation of the spine, vertical motion of the viscera, axial and shear deformation of the buttocks tissue and rotation of the pelvis. Therefore, it was assumed that the model required to predict motion of the whole body would be one consisting of the spinal column with the curvature, head, pelvis, viscera and buttocks tissue in at least the two-dimensional space of the mid-sagittal plane. The objectives of the present study are to develop a biomechanical model by comparing the vibration mode shapes of the model with those previously measured in the laboratory and to identify: (1) how the body deforms in the mid-sagittal plane, especially at the resonances seen between 4 and 6 Hz and between 8 and 12 Hz; and (2) how a change of posture (spinal curvature and rotation of the pelvis) affects the principal resonance.

2. BIOMECHANICAL MODEL

2.1. MODEL DESCRIPTION

The present model was evolved from those developed by Belytschko and Privitzer [14]. Belytschko and Privitzer assessed the accuracy of their models by using driving point impedance. However, this validation does not seem to be exhaustive, since the driving point impedance can be dominated by the motion of the seat–buttocks interface and hardly reflects the motion of other body parts, as Payne and Band [10] suggested. The present model was constructed in two dimensions in the mid-sagittal plane, although Belytschko's models were three-dimensional. The finite element method was used to model the spine, viscera, head, pelvis and buttocks tissue, using beam, spring and mass elements (see Figure 1). The geometry and material properties were based on those Belytschko and Privitzer used and also others. Some geometry and stiffness data were modified, comparing the vibration mode shapes of the model with the measurements obtained by Kitazaki and Griffin [15]. The present model was entirely linear and included 134 elements and 87 master degrees of freedom.

The spinal column was modelled by a series of beam elements according to the Simplified Spine Model (SSM) of Belytschko and Privitzer [14]. However, the present model consisted of 24 beam elements, representing all the intervertebral discs between the vertebra C1 and the sacrum S1 in contrast to only four beam elements for the SSM. All the discs were modelled separately to predict all the possible bending modes of the spine. Each spinal beam was placed between the geometrical centres of adjacent vertebral bodies, and was given the axial and bending stiffnesses of the disc. No mass was assigned to the spinal beams.

Mass elements for the torso were located anterior to the spine in the region between the T1 and T10 levels by massless rigid links, so as to model the eccentric inertial loading of the torso on the spine. Below the T10 level (the diaphragm level), the spinal masses and the visceral masses were modelled by separate mass elements. The sum of the spinal and the visceral masses at each vertebral level corresponded to the torso mass, with its mass centre also located anterior to the spine. In the cervical region, mass elements for the neck were located on the spinal beams without eccentricity. The modelling technique for the torso masses followed that used in the Isolated Ligamentous Spine with Viscera (ILSV) of Belytschko and Privitzer [14], in which each vertebra was assumed to be embedded into

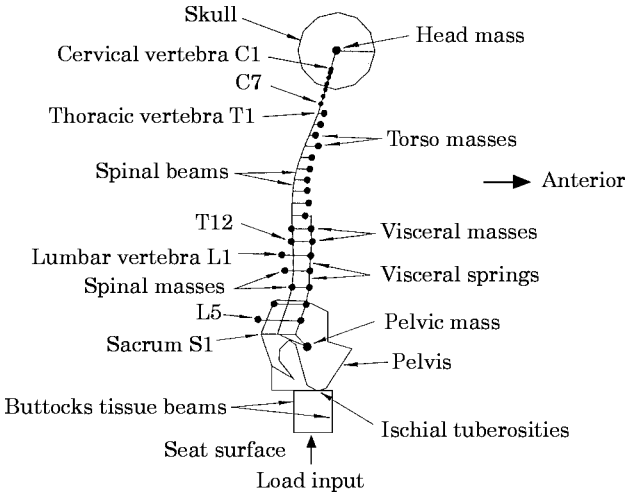

Figure 1. The two-dimensional biomechanical model in the normal posture.

the corresponding horizontal cross-sectional segment of the torso and each torso mass included all the contents within the segment.

Only the viscera below the T10 level was modelled because the mass of the viscera within the abdominopelvic cavity seemed to be larger than that within the thoracic cavity and it was thought that its local motion might affect the dynamic response of the whole body. This assumption seemed to be reasonable, upon considering the change in the impedance data measured by Coermann [1] with a tight envelope around the pelvis and the abdomen of the subject. The mass of the viscera in the thoracic cavity was included in the torso masses above the T10 level. The visceral subsystem was based on that used in the ILSV of Belytschko and Privitzer [14]. The visceral column in the abdominopelvic cavity was modelled by seven mass elements at the levels from T11 to L5 interconnected by spring elements. The bottom of the visceral column was connected to the pelvic mass by a massless rigid link, and the top connected to the spinal beam at the T10 level, also by a massless rigid link representing the pair of the lowest complete ribs. The interaction between the viscera and the spine was modelled by horizontal spring elements interconnecting the visceral masses and the spinal beams. Each visceral mass was assumed to be a mobile portion of the torso segment at each vertebral level and did not represent any specific organs. The motion of the viscera was assumed to occur only in the axial direction. This assumption may not be true. The viscera within the abdominopelvic cavity may behave like a balloon (see Belytschko *et al*. [13]). However, the assumption was adopted to simplify the subsystem for the primary interest in the vibration mode shapes of the body exposed to whole-body vertical vibration at frequencies below 10 Hz.

The head was simply modelled by a mass element based on the ILSV of Belytschko and Privitzer [14], but it was connected to the top of the spinal beam at the C1 level by a beam element representing the atlanto-occipital joint which the ILSV did not have. The pelvis was modelled by a mass element and connected to the bottom of the spinal beam at the S1 level by a massless rigid link based on the ILSV. Although the ILSV was given a single spring element beneath the pelvic mass for the buttocks tissue, two beam elements were used for the buttocks tissue in the present model so as to allow rotational and fore-and-aft motion of the pelvis as observed by Kitazaki and Griffin [15]. The beam elements were located in parallel (front and rear) beneath the pelvis and connected to the bottom of the spinal beam and the pelvic mass by massless rigid links. The limbs were not geometrically modelled but their inertial effects were included. The outline of the skull and the pelvis are drawn in Figure 1 to assist interpretation.

2.2. GEOMETRY

The spinal curves of the present model were based on the mean data of eight subjects, newly measured by using an anthropometric stand. The subjects adopted three postures: erect, normal and slouched. In the erect posture the pelvis was rotated forward with a maximally forward bent lumbar spine and an upright thoracic and cervical spine. In the normal posture the pelvis was rotated backward with a straightened lumbar spine, without moving the upper thoracic and cervical spine from the erect position. In the slouched posture the thoracic and the cervical spine inclined forward about 25 degrees from the normal position, with the same pelvic rotation as for the normal posture.

Vertical and fore-and-aft co-ordinates were measured on the posterior surface of the head and over the spinous processes of the vertebrae T1, T6, T11 and L3 and the sacrum S1 of the subjects. The location of the ischial tuberosities was also measured. The measured data were transferred to the locations of the head mass centre and the geometrical centres of the vertebral bodies based on the data of Liu and Wickstrom [16], Belytschko *et al*. [13], and Singley III and Haley [17]. The cervical spine was approximated by a straight

line drawn from the head mass centre to the geometrical centre of the vertebra T1, with the co-ordinates of the vertebrae based on the data of Belytschko *et al*. [13] with a proportional relationship. For the thoraco-lumbar spine, unmeasured co-ordinates of the vertebrae were estimated, by using the data of Belytschko *et al*. [13] and a cubic spline interpolation. The pelvic angle was determined, using the relative locations of the sacrum S1 and the ischial tuberosities.

In the region from T1 to T10, the eccentricities of the torso masses from the spinal beams were those measured by Liu and Wickstrom [16]. Below the T10 level, the locations of the visceral masses were determined arbitrarily, but the eccentricities of the spinal masses from the spinal beams were calculated so that the sum of the spinal mass and the visceral mass (translational and rotational) at each level coincided with that of the corresponding torso segment at the mass centre measured by Liu and Wickstrom [16]. The segmental masses of the neck were located on the spinal beams without eccentricity (the data of Liu and Wickstrom [16] did not include the cervical region).

The location of the pelvic mass was defined relative to the sacrum S1 and the ischial tuberosities. The pelvis was rotated around the pivot at the ischial tuberosities when changing the pelvic angle with a postural change. The location of the pelvic mass, which affected the rotational motion of the pelvis, was determined by comparing the vibration mode shapes of the rotational modes of the pelvis with the measurements obtained by Kitazaki and Griffin [15]. Node locations for the model are shown in Tables 1 and 2.

2.3. INERTIAL DATA

Inertial properties for the motion segments of the neck were based on the data of Williams and Belytschko [18]. The translational and rotational torso masses were derived from the data of Liu and Wickstrom [16] for the levels from T1 to T10. The mass of the upper arms (see the reports of NASA [19] and of McConville *et al*. [20]) was divided equally and assigned to the translational torso masses for the levels from T1 to T6. The visceral masses below the T10 level were based on ILSV of Belytschko and Privitzer [14] in which they were estimated as a mobile portion of the torso segment at each vertebral level based on the graphical data of the torso cross-sections obtained by Eycleshymer and Shoemaker [21]. The sum of the spinal mass and the visceral mass (translational and rotational) coincided with the torso mass at each level measured by Liu and Wickstrom [16]. The inertial properties of the head were based on the data from NASA [19], McConville *et al*. [20], Mawn *et al*. [22], and Singley III and Haley [17]. The pelvis was given inertial properties based on the data from NASA [19] and McConville *et al*. [20]. The translational pelvic mass was supplemented by 30% of the translational masses of the thighs, forearms and hands. The rotational pelvic mass was increased by 50%, so as to account for the additional inertia of the hands and forearms placed on the thighs. The total mass of the model was 60·046 kg. The inertial properties of the model are shown in Table 3.

2.4. STIFFNESS DATA

The geometry of the spinal beams included the vertebral bodies and the intervertebral discs, but they were given axial and bending stiffnesses of the intervertebral discs, assuming that the vertebral bodies were rigid at low frequencies. The intervertebral ligaments and articular facet interactions were not included, since no reliable data were available. The stiffness data for the spinal beams in the cervical region were based on those for the intervertebral discs and the atlanto-occipital joint estimated by Williams and Belytschko [18]. In the thoraco-lumbar region, the stiffness data were derived from the ILSV of Belytschko and Privitzer [14]. The stiffness values for the intervertebral discs in the lumbar region were increased from those obtained from isolated discs by the authors so as to

TABLE 1

Node locations for the head mass, spinal beams and pelvic mass in the three postures

	Erect posture ($m \times 10^{-2}$)		Normal posture ($m \times 10^{-2}$)		Slouched posture ($m \times 10^{-2}$)	
Level	x†	z	x	z	x	z
Head	2·983	80·863	2·570	80·250	14·856	78·157
C1	1·854	76·384	1·411	75·710	11·887	74·048
C2	1·629	75·493	1·180	74·807	11·296	73·230
C3	1·252	73·996	0·792	73·289	10·303	71·856
C4	0·877	72·507	0·407	71·780	9·316	70·490
C5	0·497	71·002	0·017	70·254	8·318	69·109
C6	0·088	69·379	−0·403	68·609	7·242	67·620
C7	−0·303	67·827	−0·805	67·036	6·214	66·196
T1	−0·694	66·275	−1·207	65·463	5·185	64·771
T2	−1·421	63·572	−2·176	62·861	3·521	62·435
T3	−2·192	60·908	−3·179	60·297	1·825	60·132
T4	−2·952	58·195	−4·179	57·686	0·124	57·786
T5	−3·608	55·474	−5·087	55·067	−1·472	55·434
T6	−4·094	52·625	−5·856	52·325	−2·930	52·971
T7	−4·296	50·032	−6·346	49·797	−4·135	50·415
T8	−4·276	47·283	−6·648	47·117	−5·085	47·705
T9	−4·036	44·411	−6·762	44·318	−5·769	44·873
T10	−3·591	41·392	−6·073	41·375	−6·202	41·897
T11	−2·969	38·250	−6·495	38·313	−6·407	38·800
T12	−2·364	35·528	−6·205	35·307	−6·436	35·622
L1	−1·792	32·519	−5·911	31·985	−6·391	32·108
L2	−1·529	29·239	−5·795	28·365	−6·437	28·280
L3	−1·961	25·748	−6·124	24·510	−6·829	24·203
L4	−3·472	21·933	−7·109	20·467	−7·742	20·077
L5	−5·522	18·202	−8·420	16·513	−8·915	16·042
S1	−7·188	15·113	−9·488	13·238	−9·871	12·700
I.T.‡	0·0	0·0	0·0	0·0	0·0	0·0
Pelvis§	−0·782	10·609	−2·436	10·355	−2·794	10·264
Pelvic angle¶	−9·02 (degrees)		0·0 (degrees)		1·99 (degrees)	

† The co-ordinate system has the x-axis for the fore-and-aft direction and the z-axis for the vertical direction with the origin at the ischial tuberosities.

‡ Ischial tuberosities.

§ Location of the pelvic mass was adjusted, comparing the vibration mode shapes.

¶ Initial pelvic angle around the pivot at the ischial tuberosities, with respect to the angle in the normal posture.

account for the effect of the cubic force–deflection relationship of the intervertebral discs and the body weight preload.

Reliable stiffness data for live tissue are difficult to obtain. Initially, the stiffness data for the viscera and the buttocks tissue were based on those used in the ILSV of Belytschko and Privitzer [14]. They determined the axial stiffnesses of the visceral springs so that the visceral resonance would coincide with that measured by Coermann *et al*. [23], assuming the torso–wall system to be a one-dimensional uniform rod. The axial stiffness of the buttocks tissue used in the ILSV was based on the model developed by Payne and Band [10]. It was divided equally and assigned to the front and rear beams of the present model. Bending deformation of the buttocks tissue beams reflected shear deformation of the tissue. Since there were no data available, their bending stiffnesses were determined by comparing the vibration mode shapes of the pelvis with the measurements obtained by Kitazaki and Griffin [15].

The axial and bending stiffnesses of the buttocks tissue beams, axial stiffnesses of the visceral springs and bending stiffnesses of the spinal beams were adjusted from the initial values mentioned above, by comparing the natural frequencies and the vibration mode shapes of the model with the measurements obtained by Kitazaki and Griffin [15]. The axial stiffnesses of the spinal beams were not altered, because axial deformation of the spine was not apparent in the measurements at frequencies below 10 Hz. The initial and the adjusted stiffnesses for the present model are shown in Tables 4, 5 and 6.

2.5. DAMPING DATA

No elemental damping was included in the present model because no reliable data were found. However, the damping effect was incorporated through the use of modal viscous damping when calculating the driving point apparent mass and the transmissibilities of the model. The modal damping ratios were determined (see Table 7), by comparing the driving point apparent mass of the model with the measurements obtained by Kitazaki and Griffin [15].

TABLE 2

Node locations for the torso masses, spinal masses and visceral masses in common for the three postures

Level	Torso or spinal mass† ($m \times 10^{-2}$)	Visceral mass† ($m \times 10^{-2}$)
C1	0·000	—
C2	0·000	—
C3	0·000	—
C4	0·000	—
C5	0·000	—
C6	0·000	—
C7	0·000	—
T1	1·351	—
T2	1·351	—
T3	1·351	—
T4	3·080	—
T5	2·500	—
T6	2·880	—
T7	2·800	—
T8	3·220	—
T9	3·810	—
T10	3·640	4·640‡
T11	−0·636	4·390
T12	−0·558	4·470
L1	−2·917	3·980
L2	−2·233	3·650
L3	−1·007	3·970
L4	−3·542	4·240
L5	−6·335	4·280
S1	—	4·280‡

† Relative horizontal co-ordinates with respect to the spinal column (vertebral body centres).

‡ Upper or lower end of the visceral column (node without a mass).

TABLE 3

Inertial properties in common for the three postures

	Torso or spinal mass		Visceral mass	
Level	Translational mass (kg)	Rotational mass† ($kgm^2 \times 10^{-2}$)	Translational mass (kg)	Rotational mass† ($kgm^2 \times 10^{-2}$)
Head	4·5	2·0	—	—
C1	0·815	0·0601	—	—
C2	0·815	0·0601	—	—
C3	0·815	0·0601	—	—
C4	0·815	0·0601	—	—
C5	0·815	0·0601	—	—
C6	0·900	0·0656	—	—
C7	1·200	0·0775	—	—
T1	2·114‡	0·0745	—	—
T2	1·829‡	0·2077	—	—
T3	1·915‡	0·2878	—	—
T4	1·819‡	0·3138	—	—
T5	1·930‡	0·3838	—	—
T6	1·948‡	0·4425	—	—
T7	1·308	0·5374	—	—
T8	1·326	0·5543	—	—
T9	1·417	0·6164	—	—
T10	1·352	0·6028	—	—
T11	0·3184	0·1283	1·282	0·5130
T12	0·3329	0·1270	1·341	0·5079
L1	0·2842	0·1036	1·676	0·5870
L2	0·3420	0·1253	1·670	0·6119
L3	0·4325	0·1482	1·720	0·5927
L4	0·5621	0·1427	1·625	0·4126
L5	0·4659	0·0993	1·774	0·3781
S1	—	—	1·708	0·1000
Pelvis	16·879§	14·13	—	—

† Rotational mass around the mass centre.
‡ Include the translational mass of the upper arms × 1/6 (0·755 kg).
§ Sum of the masses for the pelvis (10·9 kg), thighs × 0·3 (4·86 kg) and hands × 0·3 (1·119 kg).

2.6. CALCULATION CONDITIONS

The present model was constructed, and the responses were calculated, by using Ansys-PC/Linear 4.4 (Swanson Analysis Systems, Inc.) on a PC computer. The master degrees of freedom were defined as the vertical, fore-and-aft and rotational directions at all the masses, except at the visceral masses where they were defined as the direction along the visceral springs. The modal analysis was conducted first to calculate the natural frequencies and the vibration mode shapes. In the subsequent harmonic response analysis the mode-superposition method was used to calculate the driving point apparent mass and the transmissibilities. In the harmonic response analysis, the vertical force was applied to the node at the middle of the span of the horizontal rigid link connecting the lower ends of the buttocks tissue beams, and the accelerations of the driving point and other body parts were calculated. The calculated apparent mass was normalized by dividing it by sitting weight (i.e., the total mass of the model), as proposed by Fairley and Griffin [2].

3. CALCULATION RESULTS

After the adjustment of some geometry and the stiffness data (see Table 8), the model produced seven modes below 10 Hz. At these frequencies, the calculated mode shapes in the normal posture generally showed good agreement with measurements in the same posture obtained by Kitazaki and Griffin [15] (see Figure 2). The normalized apparent mass calculated with no damping (see Figure 3) indicated that the fourth mode at 5·06 Hz and the seventh mode at 8·96 Hz corresponded to the principal and the second principal resonances of the driving point apparent mass. The sixth mode at 7·51 Hz also appeared to make some contribution to the second principal resonance. The fourth mode consisted of an entire body mode, in which the head, spinal column and the pelvis move almost rigidly, with axial and shear deformation of the buttocks tissue in phase with a vertical visceral mode. The sixth and seventh modes were combinations of the second visceral mode and a rotational mode of the pelvis, with different locations of the pivot. The second visceral mode was dominant in the sixth mode, whereas the rotational mode of the pelvis was dominant in the seventh mode.

The principal resonance at about 5 Hz consisted of an entire body mode caused by deformation of the buttocks tissue and a visceral mode. Therefore, only changing parameters affecting these two modes would be expected to realize the resonance shift

TABLE 4

Stiffness data for the spinal beams of the model in common for the three postures (*initial and adjusted values*)

	Initial values		Adjusted values	
Level	Axial stiffness ($N/m \times 10^6$)	Bending stiffness ($Nm \times 10^2$)	Axial stiffness ($N/m \times 10^6$)	Bending stiffness ($Nm \times 10^2$)
Head–C1	0·550	0·40	0·550	$10 \times 0{\cdot}40$
C1–C2	0·300	0·90	0·300	$10 \times 0{\cdot}90$
C2–C3	0·700	0·08	0·700	$10 \times 0{\cdot}08$
C3–C4	0·760	0·10	0·760	$10 \times 0{\cdot}10$
C4–C5	0·794	0·12	0·794	$10 \times 0{\cdot}12$
C5–C6	0·967	0·16	0·967	$10 \times 0{\cdot}16$
C6–C7	1·014	0·22	1·014	$10 \times 0{\cdot}22$
C7–T1	1·334	0·37	1·334	$10 \times 0{\cdot}37$
T1–T2	0·70	0·20	0·70	$7 \times 0{\cdot}20$
T2–T3	1·20	0·40	1·20	$7 \times 0{\cdot}40$
T3–T4	1·50	0·60	1·50	$7 \times 0{\cdot}60$
T4–T5	2·10	1·00	2·10	$7 \times 1{\cdot}00$
T5–T6	1·90	1·00	1·90	$7 \times 1{\cdot}00$
T6–T7	1·80	1·00	1·80	$7 \times 1{\cdot}00$
T7–T8	1·50	1·00	1·50	$7 \times 1{\cdot}00$
T8–T9	1·50	1·10	1·50	$7 \times 1{\cdot}10$
T9–T10	1·50	1·10	1·50	$7 \times 1{\cdot}10$
T10–	1·50	1·20	1·50	$7 \times 1{\cdot}20$
T11–	1·50	1·00	1·50	$7 \times 1{\cdot}00$
T12–L1	1·80	0·90	1·80	$7 \times 0{\cdot}90$
L1–L2	2·13	0·90	2·13	$7 \times 0{\cdot}90$
L2–L3	2·00	0·90	2·00	$7 \times 0{\cdot}90$
L3–L4	2·00	0·90	2·00	$7 \times 0{\cdot}90$
L4–L5	1·87	0·80	1·87	$7 \times 0{\cdot}80$
L5–S1	1·47	0·70	1·47	$1 \times 0{\cdot}70$

TABLE 5

Stiffness data for the visceral springs in common for the three postures; values were not altered after the adjustment except those for the horizontal springs

Level	Axial stiffness ($N/m \times 10^4$)
T10–T11	2·86
T11–T12	2·62
T12–L1	2·42
L1–L2	2·24
L2–L3	1·91
L3–L4	1·64
L4–L5	1·68
L5–S1	1·29
Horizontal springs (all)	Initial value = 1·00 Adjusted value = 3·00

TABLE 6

Stiffness data for the buttocks tissue beams of the model in the normal posture (initial and adjusted values)

	Initial values		Adjusted values	
Buttocks tissue beam	Axial stiffness ($N/m \times 10^4$)	Bending stiffness ($Nm \times 10^2$)	Axial stiffness ($N/m \times 10^4$)	Bending stiffness ($Nm \times 10^2$)
Front	$0{\cdot}5 \times 6{\cdot}55$	—	$0{\cdot}15 \times 6{\cdot}55$	0·04913
Rear	$0{\cdot}5 \times 6{\cdot}55$	—	$1{\cdot}2 \times 6{\cdot}55$	0·04913

associated with a change of posture. It was found that the model could only achieve the resonance shift in the apparent mass associated with a change of posture, by changing the axial stiffnesses of the buttocks tissue beams. Multiplying the axial stiffnesses of the front and rear buttocks tissue beams for the normal posture by factors of 2·0 and 0·6 achieved almost the desired shifts of the natural frequency for the principal mode in the erect and slouched postures: the calculated natural frequencies were 5·25 and 4·53 Hz for the erect

TABLE 7

The modal damping ratios used for calculating the driving point apparent mass and the transmissibilities of the model in common for the three postures

Mode number	Damping ratio
1	0·5
2	0·5
3	0·5
4	0·3
5	0·3
6	0·2
7	0·2
8 and higher	0·3

TABLE 8

Adjusted parameters and their effects on the modes below 10 Hz *in the normal posture* (**, *there was a large effect and the parameter was determined based on a comparison with the measurements*; *, *there was some effect*)

Adjusted parameter	Mode number						
	1	2	3	4	5	6	7
Location of the pelvic mass						*	**
Axial stiffness of the buttocks				**†		*	**‡
Bending stiffness of the buttocks	*	*	*		*		**
Axial stiffness of the viscera				**		*	
Bending stiffness of the spine	*	*	*		**§		**¶

† For the rear beam.
‡ For the front beam.
§ For the entire spine.
¶ For the lowest spine.

and slouched postures, whereas they were found at 5·2 and 4·4 Hz by Kitazaki and Griffin [15] in their measurements. The shifts of the natural frequency shifted the principal resonance of the apparent mass (see Figure 4).

4. DISCUSSION

The first mode of the model was fore-and-aft motion of the head and the entire spine with the pelvis still caused by a bending deformation of the spine and it corresponded to the first mode of a beam with the lower end fixed. The second and the third modes were fore-and-aft motion of the head and the pelvis in opposite phase and in phase respectively caused by bending deformations of the spine. The second and the third modes corresponded to the first and the second modes of a beam with both ends free. The natural frequencies for the first three modes of the model were significantly lower than the corresponding modes in the measurements obtained by Kitazaki and Griffin [15]. In the experiment, the extracted modal properties were less reliable below 5 Hz due to low coherencies, so the bending stiffnesses for the spinal beams of the present model were adjusted by comparing mainly the fifth mode of the model and the measurements (see Table 8). Therefore, the calculated natural frequencies for the first three modes might be considered to be more reliable than the measurements. The response levels of the first three modes were small (see Figure 3) and, therefore, the deformation magnitudes were also small.

The fourth mode was the principal mode and it consisted of an entire body mode with axial and shear deformation of the buttocks tissue in phase with a vertical visceral mode. The visceral stiffnesses, determined from a comparison of the principal mode in the calculation and in the measurements, were eventually the same as those used in the ILSV of Belytschko and Privitzer [14]. The axial stiffness of the buttocks tissue (total axial

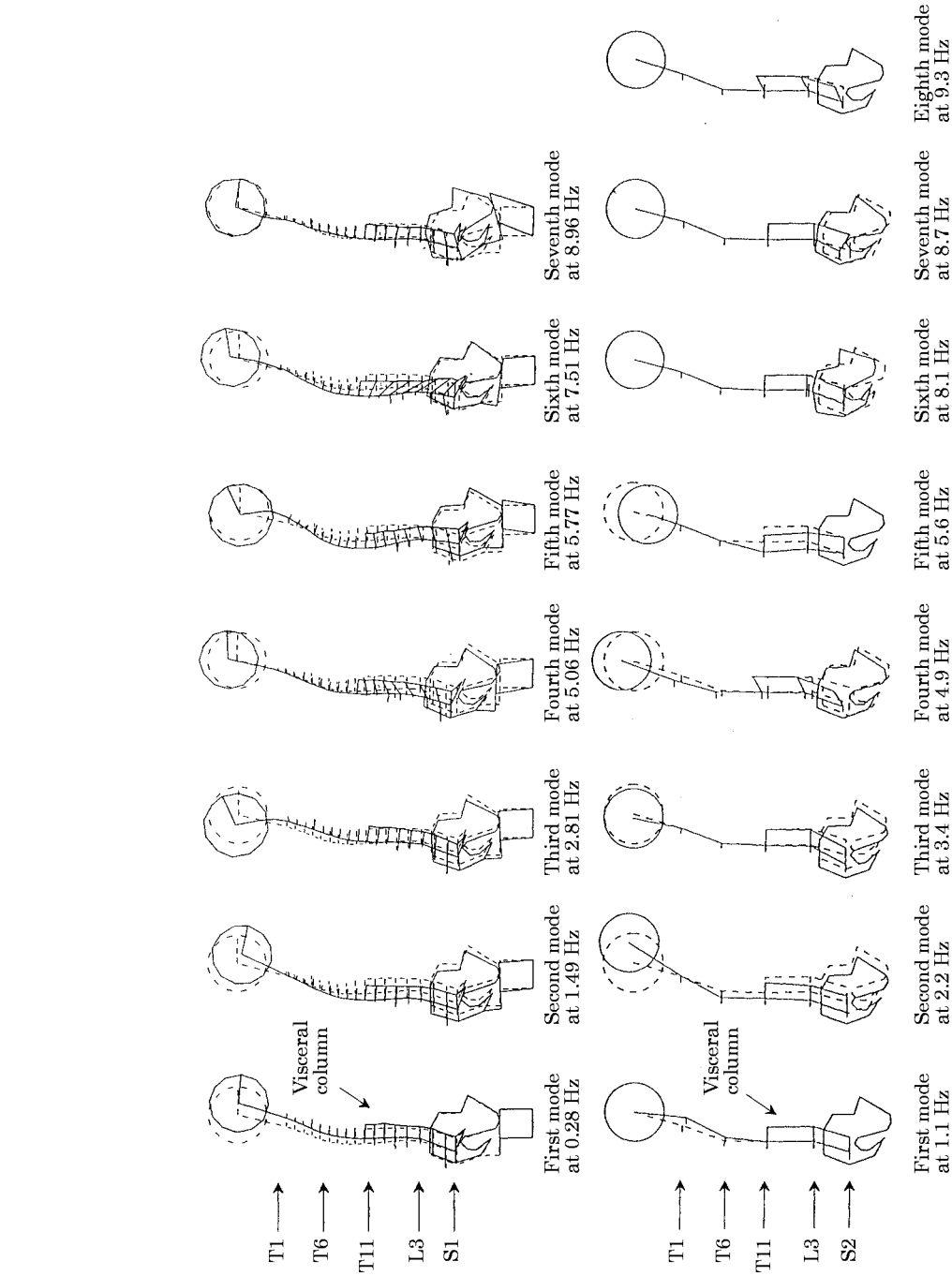

Figure 2. Calculated mode shapes (upper) and mode shapes measured by Kitazaki and Griffin [15] (lower) below 10 Hz in the normal posture: deformation (——) and initial configuration (– – – –).

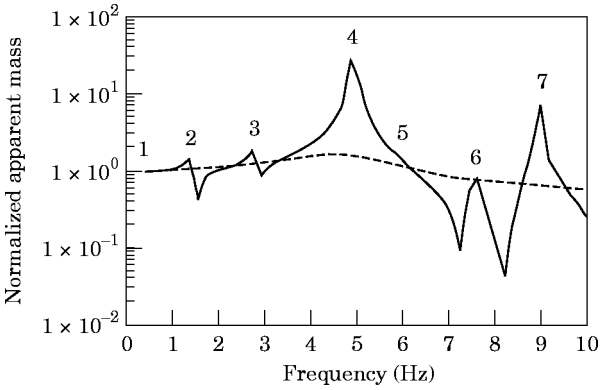

Figure 3. Normalized apparent mass of the model in the normal posture with no damping (——) and with the appropriate damping (– – – –): mode numbers are shown.

stiffness of the front and rear beams) corresponded to a 35% increase from that used in the ILSV.

The fifth mode was a bending mode of the entire spine with fore-and-aft motion of the pelvis and shear deformation of the buttocks tissue (in the measurements, the bending mode of the entire spine was separated into bending of the upper spine in the fourth mode and bending of the lower spine in the fifth mode, due to extraction errors). A pitching mode of the head was also seen in the fifth mode. The bending stiffnesses of the spinal beams were increased so as to obtain the fifth mode between 5·5 and 6 Hz, as observed in the experiment. The largest factor multiplied to the initial bending stiffnesses of the spine was ten. The initial values were principally based on force–deflection data of isolated intervertebral discs which were measured with large quasi-static deflections. Therefore, a large increment in stiffness may be reasonable for vibration conditions with small magnitudes (see the paper by Harris and Stevenson [24]). Other elastic elements connecting the vertebrae, such as ligaments and muscles may also increase the stiffness.

A rotational mode of the pelvis was found in both the sixth and seventh modes, but it was more dominant in the seventh mode. In the measured sixth and seventh modes, the lower lumbar spine below L3 appeared to deform axially with the pelvic rotation. However, the model achieved the pelvic rotation with no axial deformation of the lumbar spine by assigning a lower bending stiffness for the lowest spine and adjusting the location

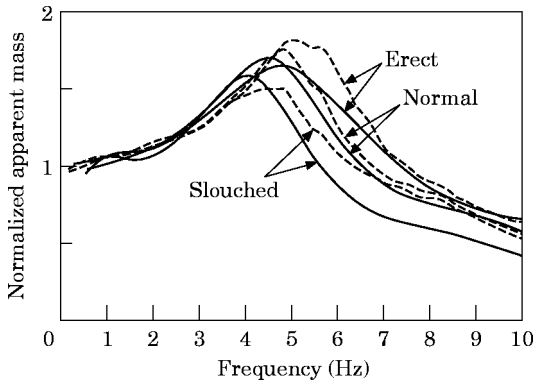

Figure 4. Normalized apparent masses of the model calculated in the three postures (——) and the normalized apparent masses in the same postures measured by Kitazaki and Griffin [15] (– – – –).

of the pelvic mass, axial and bending stiffnesses for the buttocks tissue beams (see Table 8). This result is consistent with the suggestion made by Sandover and Dupuis [5] that bending deformation of the lumbar spine and the pelvic rotation might appear as axial motion on the posterior body surface due to the depth of the lumbar spine below the posterior body surface.

In the model, both the sixth and seventh modes also included the second visceral mode, but it was more dominant in the sixth mode. The second visceral mode was vertical motion of the viscera in opposite phase to the axial deformation of the buttocks tissue. The second principal resonance appeared to correspond to the dominant rotational mode of the pelvis in the seventh mode. However, the second visceral mode in the sixth and seventh modes might also make some contribution. In the measurements, the second visceral mode was found on its own in the ninth mode at 9·3 Hz. This discrepancy might have been caused by the variability between the subjects in the measurements and also by the fact that the acceleration was measured at only one site on the abdominal wall (at the L2 level). The visceral subsystem was modelled by lumped masses interconnected by springs and the motion was assumed to occur only in the axial direction. The simplification of the viscera in the model might also be a cause of the discrepancy.

The mode shape found at the principal resonance in this study coincided with the hypothesis of Hagena *et al*. [4]. Sandover and Dupuis [5] and Hinz *et al*. [6] suggested that the principal resonance included a bending mode of the lumbar spine. However, in this study, a bending mode of the entire spine was found in the fifth mode which seemed to make a minor contribution to the principal resonance (see Figure 3). The fourth and fifth modes were located close to each other and the two modes might have been extracted together by the authors due to the heavy damping of the body. The rotational mode of the pelvis was found neither in the fourth mode nor in the fifth mode in contrast to the hypothesis of Sandover and Dupuis [5]. The mode shape found at the second principal resonance in this study did not coincide with the hypothesis of Hagena *et al*. [4].

The modes calculated above 10 Hz included higher bending modes of the spine, although they were not valid. The mode shapes were extracted only below 10 Hz by Kitazaki and Griffin [15] because higher modes were not clear due to the heavy damping of the body. The calculation also indicated that the wavelength of the spine above 10 Hz tended to be too short to measure the deformation precisely by the accelerometer positions in the experiment. The axial modes of the spine were calculated by increasing the bending stiffnesses of the spinal beams to constrain the bending deformation of the spine. The lowest axial mode of the spine was found at 16·21 Hz (see Figure 5), with deformation in the cervical and upper thoracic spine. The axial stiffnesses of the spinal beams were not altered from the initial values. However, the stiffnesses could be larger and the natural frequency for the lowest axial mode could be higher due to the same mechanisms that lead to an increase in the bending stiffnesses of the spine.

The calculated mode shapes for the principal resonance are compared in the three postures (see Figure 6). The calculated natural frequencies for the principal mode were 5·25, 5·06 and 4·53 Hz in the erect, normal and slouched postures, respectively. The natural frequencies extracted from the measured apparent masses in the three corresponding postures were 5·2, 4·9 and 4·4 Hz. It was hypothesized that changing posture from erect to slouched would increase the effective contact areas between the buttocks and thighs and the seat surface, resulting in a decrease in the total axial stiffness under the pelvis due to the non-linear force–deflection relationship of tissue (see the report by Payne and Band [10]). The resonance shift was larger when changing from the normal posture to the slouched posture than when changing from the erect posture to the normal posture. This may be explained if the backward rotation of the pelvis from the erect posture to the

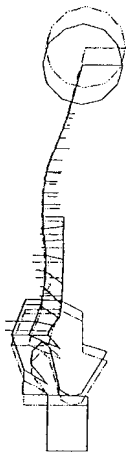

Figure 5. The lowest axial mode of the spine of the model in the normal posture at 16·21 Hz (calculated by constraining the bending deformation of the spine).

normal posture increases contact of some part of the buttocks posterior to the ischial tuberosities, and if the forward inclination of the thoraco-cervical spine and the head from the normal posture to the slouched posture increases contact with the thighs.

Fore-and-aft pelvic motion in the entire body mode, caused by shear deformation of the buttocks tissue, increased when changing posture from erect to slouched (see Figure 6). The increase in the fore-and-aft pelvic motion might be caused by the increased horizontal distance between the mass centre of the entire body and the excitation point, which induced an excitation moment. The increase in shear deformation of the buttocks tissue might also contribute to the decrease in the natural frequency for the entire body mode and the principal resonance frequency, due to the much lower shear stiffness than axial stiffness of tissue (Kitazaki and Griffin [25]). This hypothesis was supported by a calculation: when the shear deformation of the buttocks tissue was constrained by increasing the bending stiffnesses for the buttocks tissue beams by five-fold, the natural frequency for the entire body mode in the slouched posture increased from 4·53 Hz to 4·75 Hz.

Various responses of the present model were compared below 10 Hz with experimental data reported in the literature (see Figures 7–11). The model responses generally show good

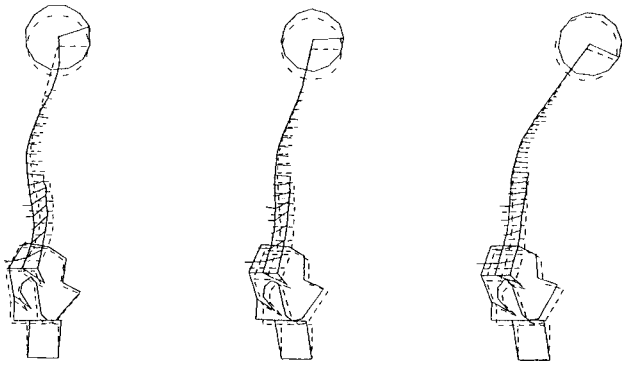

Figure 6. The mode shapes of the principal mode of the model in the three postures; (a) mode at 5·25 Hz in the erect posture; (b) mode at 5·06 Hz in the normal posture; (c) mode at 4·53 Hz in the slouched posture.

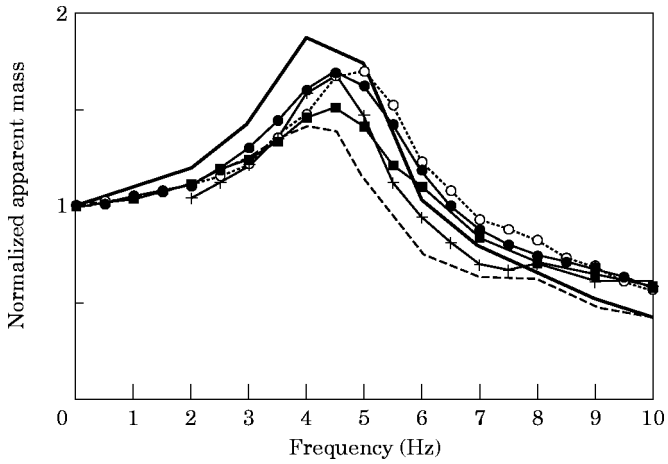

Figure 7. Normalized apparent masses: response of the model in the normal posture (—●—); mean values of eight subjects in the normal posture by Kitazaki and Griffin [15] (· · · ○ · · ·); mean values of ten subjects by Vogt *et al*. [26] (——); mean values of two subjects by Sandover [27] (– – – –); mean values of four subjects by Hinz and Seidel [28] (—┼—); mean values of 60 subjects by Fairley and Griffin [2] (—■—).

agreements with the experimental data in the apparent mass, transmissibility to vertical spinal motion and the transmissibility to vertical head motion. The transmissibility to vertical visceral motion of the model also appears to have similar trends to the measured data. In the transmissibility to fore-and-aft motion of the spine, most of the experimental data were lower than the model response at frequencies below 5 Hz. The responses of the present model above 10 Hz have not yet been validated. The model needs further validation and modification before use as a predictive tool for various responses of the body.

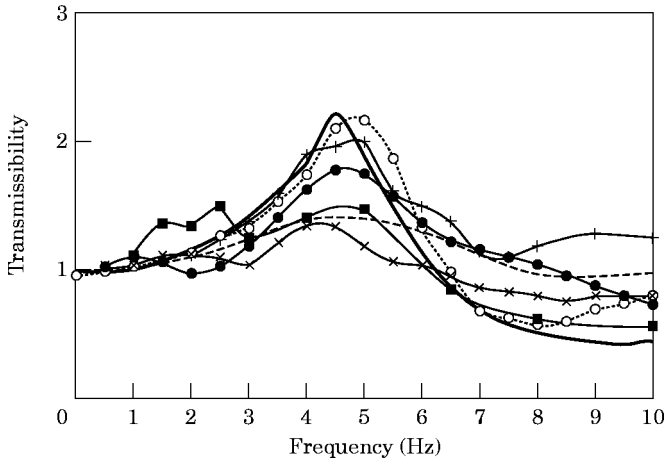

Figure 8. Acceleration transmissibilities from vertical seat motion to vertical head motion: response of the model in the normal posture (—●—); mean values of eight subjects in the normal posture by Kitazaki and Griffin [15] (· · · ○ · · ·); values of a single subject by Coermann [1] (——); mean values of 18 subjects by Griffin *et al*. [29] (—■—); median values of 12 subjects by Paddan and Griffin [30] (—×—); mean values of four subjects by Hinz and Seidel [28] (—┼—); International Standard 7962 [31] (– – – –).

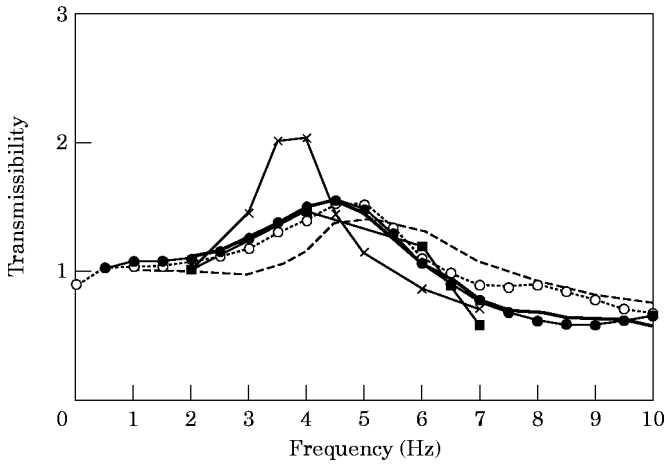

Figure 9. Transmissibilities from vertical seat motion to vertical spinal motion: acceleration (displacement) transmissibility to the vertebra L3 of the model in the normal posture (—●—); mean acceleration transmissibility to the vertebra L3 of eight subjects in the normal posture by Kitazaki and Griffin [15] (· · · ○ · · ·); mean acceleration transmissibility of the vertebra L3 of five subjects by Panjabi *et al*. [32] (——); displacement transmissibility to the vertebra L3 of a single subject by Pope *et al*. [33] (—■—); displacement transmissibility to the vertebra L4 of a single subject by Sandover and Dupuis [5] (—×—); mean acceleration transmissibility to the vertebra L3 of three subjects by Magnusson *et al*. [34] (– – – –).

5. CONCLUSIONS

A two-dimensional distributed parameter model of biomechanical response to vertical whole-body vibration has been developed. A total of seven modes was calculated for a normal body posture below 10 Hz, and the mode shapes of the model coincided well with those obtained from measurements. The fourth mode at 5·06 Hz (in the normal posture) corresponded to the principal resonance seen in the driving point response of the seated body. This consisted of an entire body mode with vertical and fore-and-aft pelvic motion

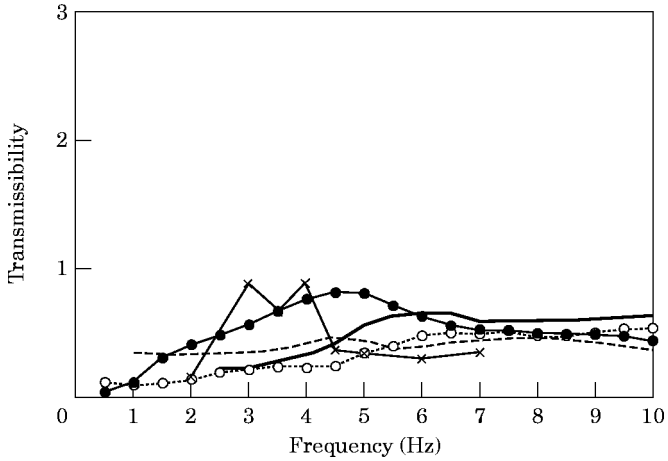

Figure 10. Transmissibilities from vertical seat motion to fore-and-aft spinal motion: acceleration (displacement) transmissibility to the vertebra L3 of the model in the normal posture (—●—); mean acceleration transmissibility to the vertebra L3 of eight subjects in the normal posture by Kitazaki and Griffin [15] (· · · ○ · · ·); mean acceleration transmissibility to the vertebra L3 of five subjects by Panjabi *et al*. [32] (——); displacement transmissibility to the vertebra L4 of a single subject by Sandover and Dupuis [5] (—×—); mean acceleration transmissibility to the vertebra L3 of three subjects by Magnusson *et al*. [34] (– – – –).

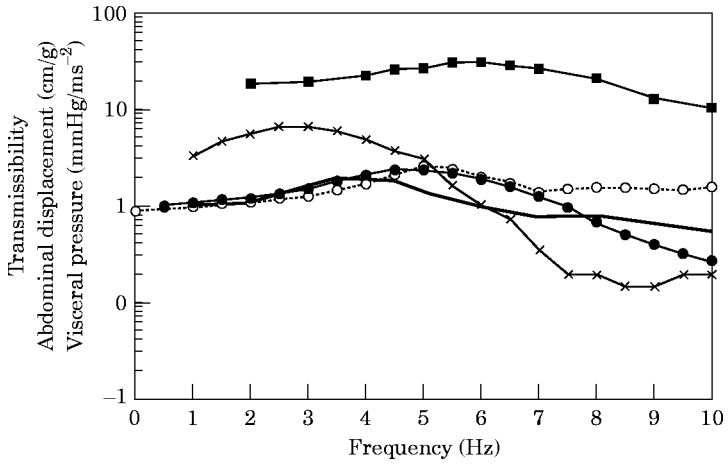

Figure 11. Responses of the viscera: acceleration (displacement) transmissibility from vertical seat motion to vertical visceral motion at the L3 level of the model in the normal posture (—●—); mean acceleration transmissibility from vertical seat motion to vertical visceral motion at the L2 level of eight subjects in the normal posture Kitazaki and Griffin [15] (· · · ○ · · ·); longitudinal abdominal wall displacement of a single subject by Coermann *et al*. [23] (— × —); mean colon pressure of eight subjects by White *et al*. [35] (——); intra-abdominal pressure of a single subject by Sandover [27] (—■—).

due to deformation of tissue beneath the pelvis occurring in phase with a vertical visceral mode. Some workers have hypothesized that the principal resonance might include a bending mode of the lumbar spine due to either a rotation of the pelvis or buttocks compression. However, in the model, a bending mode of the lumbar spine was included in the next higher mode at 5·77 Hz which seemed to make a minor contribution to the principal resonance, while a rotational mode of the pelvis was not found in either the principal mode nor in the next higher mode. The second resonance seen in the driving point response of the body corresponded mainly to the seventh mode at 8·96 Hz, but might also have contained a contribution from the sixth mode at 7·51 Hz. Both the sixth and the seventh modes contained the second visceral mode and different rotational modes of the pelvis. The rotational mode of the pelvis was dominant in the seventh mode, whereas the second visceral mode was dominant in the sixth mode.

The shift of the principal resonance of the driving point apparent mass, when changing posture, was achieved only by changing the axial stiffness of the buttocks tissue. It is suggested that changing posture may change the contract area between the buttocks and the thighs and the seat surface, resulting in a change in the total axial stiffness under the pelvis due to the non-linear force–deflection relationship of tissue. When changing posture from erect to slouched, fore-and-aft motion of the pelvis, accompanying shear deformation of the buttocks tissue, increased in the principal mode. This may be due to an excitation moment arising from the increased horizontal distance between the centre of mass of the body and the excitation point. The increase in the shear deformation of the buttocks tissue, with a change of posture from erect to slouched, may also contribute to the decrease in the natural frequency for the principal mode, due to the much lower shear stiffness of tissue than the axial stiffness.

ACKNOWLEDGMENT

This research was supported by Nissan Motor Company Ltd, Yokosuka, Japan.

REFERENCES

1. R. R. Coermann 1962 *Human Factors* **4**, 227–253. The mechanical impedance of the human body in sitting and standing position at low frequencies.
2. T. E. Fairley and M. J. Griffin 1989 *Journal of Biomechanics* **22**, 81–94. The apparent mass of the seated human body: vertical vibration.
3. M. M. Panjabi, G. B. J. Andersson, L. Jorneus, E. Hult and L. Mattsson 1986 *Journal of Bone and Joint Surgery* **86-A**, 695–702. *In vivo* measurements of spinal column vibrations.
4. F. W. Hagena, C. J. Wirth, J. Piehler, W. Plitz, G. O. Hofmann and Th. Zwingers 1985 *AGARD Conference Proceedings* **378**, 1–12. *In-vivo* experiments on the response of the human spine to sinusoidal Gz-vibration.
5. J. Sandover and H. Dupuis 1987 *Ergonomics* **30**, 975–985. A reanalysis of spinal motion during vibration.
6. B. Hinz, H. Seidel, D. Bräuer, G. Menzel, R. Blüthner and U. Erdmann 1988 *Clinical Biomechanics* **3**, 241–248. Bidimensional accelerations of lumbar vertebrae and estimation of internal spinal load during sinusoidal vertical whole-body vibration: a pilot study.
7. F. Latham 1957 *Proceedings of the Royal Society* **B-147**, 121–139. A study in body ballistics: seat ejection.
8. P. R. Payne 1965 *Aerospace Medical Research Laboratory*, *Wright–Patterson Air Force Base*, *Ohio*, *Report No*. *AMRL-TR*-65–127. Personnel restraint and support system dynamics.
9. C. W. Suggs, C. F. Abrams and L. F. Stikeleather 1969 *Ergonomics* **12**, 79–90. Application of a damped spring–mass human vibration simulator in vibration testing of vehicle seats.
10. P. R. Payne and E. G. U. Band 1971 *Aerospace Medal Research Laboratory*, *Wright–Patterson AirForce Base*, *Ohio*, *Report No*. *AMRL-TR*-70–35. A four-degree-of-freedom lumped parameter model of the seated human body.
11. R. Toth 1966 *Engineering in Medicine and Biology*, *Proceedings of the* 19*th Annual Conference*, 102. Multiple degree-of-freedom, nonlinear spinal model.
12. D. Orne and Y. K. Liu 1971 *Journal of Biomechanics* **4**, 49–71. A mathematical model of spinal response to impact.
13. T. Belytschko, L. Schwer and A. Schultz 1976 *Aerospace Medical Research Laboratory*, *Wright–Patterson Air Force Base*, *Ohio*, *Report No*. *AMRL-TR*-76–10. A model for analytic investigation of three dimensional head–spine dynamics.
14. T. Belytschko and E. Privitzer 1978 *Aerospace Medical Research Laboratory*, *Wright–Patterson Air Force Base*, *Ohio*, *Report No*. *AMRL-TR*-78–7. Refinement and validation of a three-dimensional head–spine model.
15. S. Kitazaki and M. J. Griffin 1996 Awaiting publication. Resonance behaviour of the seated human body and effects of posture.
16. Y. K. Liu and J. K. Wickstrom 1973 *Perspectives in Biomedical Engineering*, *Proceedings of a Symposium Organised in Association with the Biological Engineering Society at Glasgow*, 1972. Estimation of the inertial property distribution of the human torso from segmented cadaveric data.
17. G. T. Singley III and J. L. Haley 1978 *AGARD Conference Proceedings* **253**(A22), 1–17. The use of mathematical modelling in crashworthy helicopter seating systems.
18. J. L. Williams and T. Belytschko 1981 *Air Force Aerospace Medical Research Laboratory*, *Wright–Patterson Air Force Base*, *Ohio*, *Report No*. *AFAMRL-TR*-81–5. A dynamic model of the cervical spine and head.
19. NASA 1978 *NASA Reference Publication* 1024. Anthropometric source book, volume 1: anthropometry for designers.
20. J. T. McConville, T. D. Churchill, I. Kaleps, C. E. Clauser and J. Cuzzi 1980 *Air Force Aerospace Medical Research Laboratory*, *Wright–Patterson Air Force Base*, *Ohio*, *Report No*. *AFAMRL-TR*-80–119. Anthropometric relationships of body and body segment inertia.
21. A. C. Eycleshymer and D. M. Shoemaker 1970 Meredith Corporation: A cross-section anatomy.
22. S. V. Mawn, J. J. Lambert and J. L. Catyb, Jr 1992 *Aviation*, *Space and Environmental Medicine* **63**, 32–36. The relationship between head and neck anthropometry and kinematic response during impact acceleration.
23. R. R. Coermann, G. H. Ziegenruecker, A. L. Wittwer and H. E. Von Gierke 1960 *Aerospace Medicine* **31**, 443–455. The passive dynamic mechanical properties of the human thorax–abdomen system and of the whole body system.

24. J. HARRIS and A. STEVENSON 1987 *Journal of Vehicle Design* **8**, 553–577. On the role of non-linearity and the dynambehaviour of rubber components.
25. S. KITAZAKI and M. J. GRIFFIN 1995 *Journal of Biomechanics* **28**, 885–890. A data correction method for surface measurement of vibration on the human body.
26. H. L. VOGT, R. R. COERMANN and H. D. FUST 1968 *Aerospace Medicine* **39**, 675–679. Mechanical impedance of the sitting human under sustained acceleration.
27. J. SANDOVER 1978 *Aviation, Space and Environmental Medicine* **49**, 335–339. Modelling human response to vibration.
28. B. HINZ and H. SEIDEL 1987 *Industrial Health* **25**, 169–181. The nonlinearity of the human body's response during sinusoidal whole body vibration.
29. M. J. GRIFFIN, C. H. LEWIS, K. C. PARSONS and E. M. WHITHAM 1978 *AGARD Conference Proceedings* **253**(A28), 1–18. The biodynamic response of the human body and its application to standards.
30. G. S. PADDAN and M. J. GRIFFIN 1993 *University of Southampton, ISVR Technical Report* 218. Transmission of vibration through the human body to the head: a summary of experimental data.
31. INTERNATIONAL ORGANIZATION FOR STANDARDIZATION 1987 *ISO* 7962, *International Organization for Standardization, Geneva*. Mechanical vibration and shock—Mechanical transmissibility of the human body in the *z* direction.
32. M. M. PANJABI, G. B. J. ANDERSSON, L. JORNEUS, E. HULT and L. MATTSSON 1986 *Journal of Bone and Joint Surgery* **68-A**, 695–702. *In vivo measurement of spinal column vibrations*.
33. M. H. POPE, M. SVENSSON, H. BROMAN and G. B. J. ANDERSSON 1986 *Journal of Biomechanics* **19**, 675–677. Mounting of the transducers in measurement of segmental motion of the spine.
34. M. MAGNUSSON, M. POPE, M. ROSTEDT and T. HANSSON 1993 *Clinical Biomechanics* **8**, 5–12. Effect of backrest inclination on the transmission of vertical vibrations through the lumbar spine.
35. G. H. WHITE, JR., K. O. LANGE and R. R. COERMANN 1962 *Human Factors* **4**, 275–290. The effects of simulated buffeting on the internal pressure of man.

APPENDIX: A SUMMARY OF EXPERIMENTAL MODAL ANALYSIS OF WHOLE-BODY VIBRATION

A.1. EXPERIMENTAL METHOD

Acceleration responses of the spine, pelvis, viscera and the head to whole-body vertical vibration in a sitting position were measured. Spinal responses were measured at four vertebrae T1, T6, T11 and L3 and at the sacrum S2. A pair of miniature accelerometers (Entran model EGA–125–10D) weighing 1 g was attached to the body surface over each spinous process via a stiff card using double-sided adhesive tape and orientated along the spine and perpendicular to the spine so as to measure the response in the mid-sagittal plane. The same type of accelerometer was attached to the pelvis on the front-upper edge of the right iliac crest. It was oriented in the vertical direction so as to determine the rotational response of the pelvis with the responses measured at the sacrum S2, assuming that the pelvis was rigid. The vertical response of the viscera was measured by attaching the same type of accelerometer on the abdominal wall at the level of L2. The responses of the head in the mid-sagittal plane were measured by accelerometers (Entran Model EGCSY–240D–10D) mounted on a bite-bar. The same type of accelerometer measured vertical acceleration of the rigid seat. The vertical force was measured by a force platform, Kistler Type 9281B, placed between the seat and the buttocks of the subjects.

Eight subjects participated in the experiment. The subjects sat on the force platform connected to the seat without a backrest mounted on a vibrator and adopted erect, normal and slouched postures. They were exposed to 1 minute of vertical random vibration (0·5–35 Hz) with a magnitude of 1·7 m/s^2 r.m.s. Posture was measured and controlled using an anthropometric stand before each run. The time histories of acceleration and force were acquired simultaneously into a computer with a sampling rate of 100 samples per second through anti-aliasing low-pass filters at 35 Hz with a cut-off rate of 36 dB/octave. The

longitudinal and vertical accelerations measured on the body surface were corrected to eliminate the effect of the local tissue–accelerometer vibration from the measurements, by using the method proposed by Kitazaki and Griffin [25]. Transfer functions between vertical seat acceleration and acceleration on the body were calculated for the modal analysis. The modal properties were extracted from the mean transfer functions of the eight subjects in each of the three postures at frequencies below 10 Hz. The method used for extraction was classified as the dynamic stiffness method. The driving point apparent masses were also calculated and then normalized, by dividing them by the sitting weights of the subjects, as proposed by Fairley and Griffin [2].

A.2. RESULTS

A total of eight modes was extracted below 10 Hz. Higher modes above 10 Hz were not clear due to the heavy damping of the body. A principal resonance of the human body at about 5 Hz was found to involve a combination of an entire body mode, in which the head, spinal column and the pelvis moves almost rigidly, with axial and shear deformation of tissue beneath the pelvis in phase with a vertical visceral mode. A bending mode of the upper thoracic and the cervical spine was also found at the principal resonance. A bending mode of the lumbar and lower thoracic spine was found with a pitching mode of the head at the next higher mode which was located close to the principal resonance. A second principal resonance, at about 8 Hz, corresponded to rotational modes of the pelvis and might contain some contribution from a second visceral mode. When a subject changed posture from erect to slouched, the natural frequency for the entire body mode decreased, resulting in a decrease in the frequency of the principal resonance of the human body at about 5 Hz. The fore-and-aft motion of the pelvis, including shear deformation of the buttocks tissue, was found to increase in the entire body mode due to the same change of posture.